

## Anion-Antisite-like Defects in III-V Compounds

M. J. Caldas,<sup>(a)</sup> J. Dabrowski,<sup>(b)</sup> A. Fazzio,<sup>(a)</sup> and M. Scheffler

Fritz-Haber-Institut, Faradayweg 4-6, D-1000 Berlin 33, Federal Republic of Germany

(Received 1 June 1990)

We report *ab initio* calculations of total energies and electronic structures of P, As, and Sb donors in GaAs and InP. In the  $T_d$  geometry, all these defects exhibit two donor states in the forbidden gap, an internal optical excitation energy of the order of 1 eV, and a Franck-Condon shift of the order of 0.1 eV. All these defects possess a metastable geometry of the electrically neutral vacancy-interstitial pair, with no donor states in the band gap. We discuss the differences between the six systems and explain why an optically inducible transition to the metastable state is inefficient for GaAs:Sb<sub>Ga</sub>.

PACS numbers: 71.55.Eq, 61.70.At, 71.45.Nt

As theoretical studies have shown, the As-antisite defect in GaAs exhibits a structural metastability (Fig. 1).<sup>1-3</sup> In fact, it has been suggested<sup>3</sup> that all cation-site double donors in zinc-blende-structure semiconductors exhibit a structural metastability similar to that of GaAs:As<sub>Ga</sub>. However, no metastable properties have been observed experimentally for analogous systems (see, for example, Refs. 4 and 5).

In this paper we show that the structural metastability (sketched in Fig. 1) is indeed an intrinsic property of anion-antisite-like defects in III-V semiconductors. However, we argue that the optically inducible transformation to the metastable configuration will be inefficient for Sb<sub>Ga</sub> in GaAs. Furthermore, we investigate the influence of lattice relaxation. In particular, for Sb<sub>Ga</sub> in GaAs we find that the lattice relaxation causes a significant localization of the bound-state electrons.

Our conclusions are based on density-functional-theory (DFT) calculations for six antisite and antisite-like defects (P, As, and Sb in GaAs and InP). We use a 54-atom supercell, separable *ab initio* pseudopotentials,<sup>6,7</sup> and a plane-wave basis set with a cutoff energy of 8 Ry. Electron densities are evaluated from the states at  $\Gamma$ . For the calculation of donor energies and Franck-Condon shifts we use a set of two special points. The details of the calculations will be given in a separate paper.

An anion antisite in a III-V compound is created when

a group-III atom substitutes a group-V atom of the host, and as such it should be a double donor. Antisite defects are expected to be abundant in thermodynamic equilibrium if the crystal is grown under anion-rich conditions and if the formation energy is lower than that of competing processes, namely, the formation of cation vacancies and anion interstitials.<sup>8</sup> Under nonequilibrium conditions, otherwise unlikely anion antisites (for example, InP:P<sub>In</sub>) may also be formed as a consequence of irradiation-induced cation vacancies, which may capture anion interstitials. Qualitatively, the electronic structure of a tetrahedral anion antisite can be estimated from atomic terms in a simple tight-binding model, where atomic orbitals of the substitutional atom hybridize with the dangling bonds of the cation vacancy.<sup>9,10</sup> We then expect a deep bound state of  $A_1$  symmetry, and above it a state of  $T_2$  symmetry. If lattice relaxation is neglected, the eigenvalue  $\epsilon(a_1)$  should follow the trend of the atomic-*s*-orbital energy. Since the donor transition involves a population change in the  $a_1$  state, we then expect electronic levels to move with the atomic number towards higher energies. This is indeed the trend we observe for *unrelaxed* tetrahedral antisites, i.e., when all host atoms remain in their perfect-crystal positions [see Table I, the  $\epsilon(a_1)$  and (+/0) results in parentheses]. The  $t_2$  state, on the other hand, is found to be resonant in the conduction band and its position is more closely related to the band structure of the host.

When a substitutional defect is created, the neighboring atoms relax from their perfect-crystal sites.<sup>11</sup> We find that the breathing relaxation of the neutral anion antisites increases the anion-anion bond length (except for InP:P<sub>In</sub><sup>0</sup>, which shows a small inwards relaxation; see  $\Delta Q$  in Table I). Because of the antibonding character of the  $a_1$  state, the increase in the bond length can cause an increase of localization of the wave function. The largest effect is found for Sb<sub>Ga</sub><sup>0</sup> (compare the two lower contour plots in Fig. 2), which has the most delocalized  $a_1$  state among the anion antisites in GaAs, as is clearly seen in Fig. 2. The difference  $\Delta\epsilon = \epsilon(t_2) - \epsilon(a_1)$  increases with the localization of both states. This is reflected in the

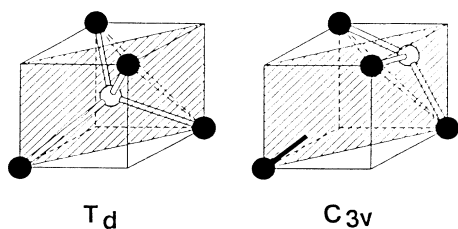


FIG. 1. Stable ( $T_d$ ) and metastable ( $C_{3v}$ ) geometries of anion-antisite-like defects. Solid circles are the crystal-lattice anions; the open circle is the defect atom. The (110) plane is shown by the hatch lines.

TABLE I. Calculated Franck-Condon shifts  $E_{FC}$ , single-particle eigenvalues  $\epsilon(a_1)$  with respect to the top of the valence band, donor levels (+/0), optical excitation energies  $E_o$ , relaxation energies  $E_{rel}$ , barrier heights  $E_W$ , and metastable energies  $E_M$  for different anion-antisite defects in the tetrahedral ( $T_d$ ) and vacancy-interstitial pair (VI,  $C_{3v}$ ) atomic configurations in GaAs and InP. Electronic levels (+/0) =  $E(+)-E(0)+E_F$  are calculated from total-energy differences using two special  $\mathbf{k}$  points, and refer to  $E_F$  at the valence-band top.  $E_{rel}$  denotes the energy gained by the breathing relaxation of the first four atomic neighbors from the perfect-crystal position, and  $\Delta Q$  gives the distance each atom moves.  $E_W$  is the energy barrier from the stable  $T_d$  to the VI configuration,  $E_M$  is the energy difference between the  $T_d$  and VI geometries, while  $Q_M$  gives the distance from the  $T_d$  lattice site to the VI site (Ref. 16). Values in parentheses correspond to unrelaxed atomic positions. All results refer to neutral defects.

	$E_{FC}$ (eV)	$T_d$ atomic configuration			$E_{rel}$ (eV)	$\Delta Q$ (Å)	Barrier		VI	
		$\epsilon(a_1)$ (eV)	(+/0) (eV)	$E_o$ (eV)			$E_W$ (eV)	$E_M$ (eV)	$Q_M$ (Å)	
GaAs:										
P	0.05	0.24 (0.52)	0.71 (0.88)	1.16 (1.06)	0.20	0.10	0.9 (0.9)	0.3 (0.3)	1.4 (1.4)	
As	0.03	0.25 (0.63)	0.81 (1.05)	0.97 (0.91)	0.42	0.12	0.7 (0.8)	0.4 (0.2)	1.2 (1.2)	
Sb	0.04	0.43 (1.17)	0.95 (1.75)	1.03 (0.31)	1.71	0.27	1.2 (0.6)	0.5 (-0.4)	1.4 (1.6)	
InP:										
P	0.10	0.68 (0.57)	0.95 (0.78)	1.50 (1.36)	0.01	-0.03	(1.4)	(0.6)	(1.3)	
As	0.09	0.55 (0.67)	1.3 (1.2)	1.32 (1.20)	0.00	0.01	(1.2)	(0.5)	(1.4)	
Sb	0.08	0.75 (1.18)	1.3 (1.6)	0.77 (0.72)	0.48	0.14	(1.0)	(0.4)	(1.3)	

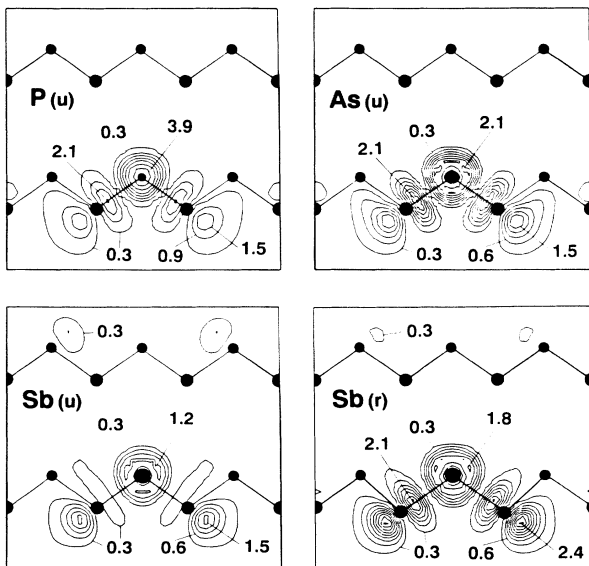


FIG. 2. Neutral anion-antisite-like defects in GaAs: squared single-particle wave function of the filled  $a_1$  state for the *unrelaxed* defects  $P_{Ga}$  [upper left panel, labeled  $P(u)$ ],  $As_{Ga}$  [upper right panel,  $As(u)$ ], and  $Sb_{Ga}$  [lower left panel,  $Sb(u)$ ], and for the *relaxed*  $Sb_{Ga}$  [lower right panel,  $Sb(r)$ ]. Units are electrons per bulk GaAs unit-cell volume; the distance between the contour lines is 0.6 for  $P_{Ga}$  and 0.3 for  $As_{Ga}$  and  $Sb_{Ga}$ .

corresponding increase of the internal optical excitation energy  $E_o$  (see Fig. 3 and Table I), which is related to  $\Delta\epsilon$  as we will discuss below.

If one of the two  $a_1$  electrons is removed, the bonds are strengthened because of the antibonding character of the deep-level wave function and because the electrostatic interaction between the negatively charged neighbors (anions) and the positively charged antisite will move the neighbors closer to the defect atom. The dependence of the relaxation of the four nearest neighbors on the charge state of the defect gives rise to a Franck-Condon shift ( $E_{FC}$  in Table I). As expected from this discussion, the shifts are bigger for defects in more ionic InP than for defects in less ionic GaAs. Our result for  $As_{Ga}$  in GaAs (0.03 eV) is much smaller than the experimental value of 0.12 eV found for  $EL2$ .<sup>12</sup> However, it should be noted that the effect of long-range relaxation has not been considered (for a more detailed discussion of this point, see Ref. 13).

In close similarity to the  $As_{Ga}$  defect in GaAs,<sup>1,3</sup> we find that all the anion-antisite defects investigated here possess *in the neutral charge state* a metastable minimum in the total-energy surface, with the defect atom displaced along the  $\langle 111 \rangle$  axis, roughly halfway between the substitutional site and the closest  $T_d$  interstitial site (Figs. 1 and 3).

The displacement of the antisite atom lowers the local

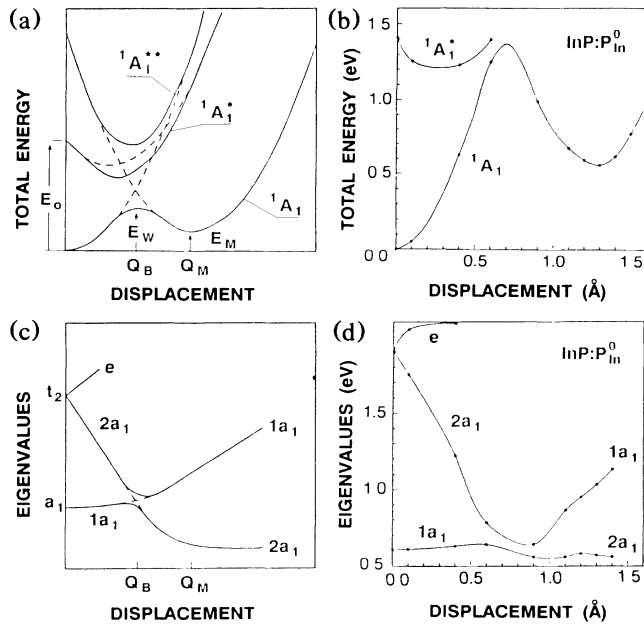


FIG. 3. Single-particle energies (bottom) and total energies for the ground and excited electronic configurations (top) as a function of the displacement of the defect atom along the  $\langle 111 \rangle$  axis. Left: schematic description. Right: results of calculations for  $\text{InP:P}_{\text{In}}^0$ .

symmetry to  $C_{3v}$ , and the single-particle  $t_2$  state splits:  $t_2 \rightarrow a_1 + e$ . The lowest-energy mean-field configurations of  $A_1$  symmetry are then  $(1a_1^2 2a_1^0)$ ,  $(1a_1^1 2a_1^1)$ , and  $(1a_1^0 2a_1^2)$ , which may interact to yield three non-paramagnetic states ( $S=0$ ):  ${}^1A_1$ ,  ${}^1A_1^*$ , and  ${}^1A_1^{**}$ . In Fig. 3(a) we depict the dependence of the total energies on the displacement  $Q$  of the impurity for these three states. We also show in a schematic form the typical behavior of the single-particle eigenvalues [Fig. 3(c)]. For small displacements  $Q$  the energy of the ground state exhibits a parabolic behavior around the minimum at the  $T_d$  site, and is dominated by the configuration  $(1a_1^2 2a_1^0)$ . With further displacement, the eigenvalue difference  $\epsilon(2a_1) - \epsilon(1a_1)$  decreases and the interaction between the three configurations increases until we reach the anticrossing point which results in the local maximum of the ground-state energy at  $Q_B$ . In this process the occupied  $a_1$  state localizes and evolves into a dangling-bond state at the cation vacancy. The usual way to picture this configuration interaction is shown in Fig. 3(a), where to the right of  $Q_B$  the dominant configuration of the ground state is ascribed to the configuration  $(1a_1^0 2a_1^2)$ . In Figs. 3(b) and 3(d) we plot our results for the system  $\text{InP:P}_{\text{In}}^0$ , with fixed neighbor positions. We have calculated the total energy for the two lowest-energy mean-field configurations, which are labeled as  ${}^1A_1$  and  ${}^1A_1^*$ . Even though we are working within the local-density approximation, one can expect<sup>14</sup> in this case to obtain good estimates of the true correlated energies.

If the four neighbors of the defect are allowed to relax, the details of the described picture change, but the qualitative behavior remains the same. The internal optical excitation energy  $E_o$  of the  $T_d$  antisite (Fig. 3) is not much affected (Table I), while the donor levels shift slightly to lower energy (Table I). The barrier height  $E_B = E_W - E_M$  decreases (Table I). An interesting result is that in the metastable configuration  $Q_M$ , the donor levels of the six studied defects shift into the valence band. We cannot exclude that in some cases—especially in InP—there may be an acceptor level below the bottom of the conduction band.<sup>13</sup>

The  $\text{GaAs:Sb}_{\text{Ga}}$  center is particularly interesting because here the lattice relaxation results in *qualitative* changes of the defect properties. The unrelaxed  $\text{Sb}_{\text{Ga}}$  follows the chemical trends described above, but it is an extreme case: At the  $T_d$  site its  $a_1$  single-particle eigenvalue is very high, the wave function of this state is quite delocalized (Fig. 2), and the optical excitation energy  $E_o$  is very small (Table I). The difference in size between the impurity (Sb) and the removed atom (Ga) makes the VI geometry energetically more favorable, i.e.,  $E_M < 0$  (Table I). However, after the lattice relaxes, the situation is changed. The most prominent changes occur in the  $T_d$  configuration, where the Sb atom was squeezed between its four neighbors: These neighbors relax outwards by about  $0.3 \text{ \AA}$ , which gives a gain of  $1.7 \text{ eV}$ . The  $a_1$  wave function becomes more localized. The  $(+ / 0)$  electronic level shifts down in energy to  $0.95 \text{ eV}$  above the valence-band top. This is in good agreement with experimental results: Hall measurements<sup>15</sup> locate the  $(+ / 0)$  electronic level of  $\text{Sb}_{\text{Ga}}$  at  $E_V + 1.04 \text{ eV}$ . The calculated internal optical excitation energy  $E_o$  increases with the lattice relaxation to about  $1 \text{ eV}$ , which is a typical value for anion antisites in GaAs (Table I). Smaller changes are observed in the VI configuration, where the system gains about  $0.8 \text{ eV}$  relaxation energy. Because of this difference in the relaxation energy in the  $T_d$  and VI geometries, the former becomes stable, while the latter is now metastable—as is our usual result found for the other anion antisites.

The first excited state  ${}^1A_1^*$  (see Fig. 3) may provide a channel for an optically inducible transformation of a  $T_d$  antisite to its metastable VI configuration. For an observable transition to be probable we need the excited state  ${}^1A_1^*(T_d)$  to be *above* the local maximum of  ${}^1A_1$  (i.e.,  $E_o > E_W$ ). In GaAs, we find this condition fulfilled for the As and P antisites, while for the Sb antisite we obtain  $E_o < E_W$ . Hence for Sb the transition may occur only via tunneling. For InP we have calculated only the unrelaxed geometries of  $C_{3v}$  symmetry. If the lattice is relaxed, it may happen for the P antisite and the As antisite that  $E_o > E_W$ .

In conclusion, we have performed systematic DFT LDA studies of P, As, and Sb donors in InP and GaAs. In particular, we studied the effect of lattice relaxation. Whereas *before* relaxation the wave functions of dif-

ferent tetrahedral antisites have significantly different degrees of localization, they become more similar after the lattice relaxes in the breathing mode. This affects electronic excitation energies, and for GaAs:Sb<sub>Ga</sub> the lattice relaxation is essential for even *qualitative* description of this defect. For P and As in GaAs the lattice relaxation effects are less important, but must be taken into account for the correct *quantitative* description of these centers. The calculated (+/0) donor energies for the relaxed Sb and As donors in GaAs are in good agreement with experimental data for Sb<sub>Ga</sub> and EL2. Further, we find that the occupation dependence of the relaxation of the four nearest neighbors gives rise to moderate Franck-Condon shifts for all six tetrahedral defects. These shifts are bigger for more ionic InP than for less ionic GaAs. Finally, we have shown that the structural  $T_d-C_{3v}$  metastability is an intrinsic property of anion-antisite-like defects in III-V compounds. From qualitative considerations we expect that the antimony donor in GaAs exhibits a significantly smaller cross section for the *optically inducible* transition to the metastable configuration than the other above studied defects.

<sup>(a)</sup>Permanent address: Instituto de Física, Universidade de São Paulo, CP 20516, 01496 São Paulo, Brazil.

<sup>(b)</sup>Permanent address: Instytut Fizyki, Polskiej Akademii Nauk, Al. Lotników 32, 02-668 Warszawa, Poland.

<sup>1</sup>J. Dabrowski and M. Scheffler, Phys. Rev. Lett. **60**, 2183 (1988).

<sup>2</sup>D. J. Chadi and K. J. Chang, Phys. Rev. Lett. **60**, 2187

(1988).

<sup>3</sup>J. Dabrowski and M. Scheffler, Phys. Rev. B **40**, 10391 (1989).

<sup>4</sup>M. Bäuml, J. Schneider, and U. Kaufmann, W. C. Mitchell, and P. W. Yu, Phys. Rev. B **39**, 6253 (1989).

<sup>5</sup>M. Bäuml, F. Fuchs, and U. Kaufmann, Phys. Rev. B **40**, 8072 (1989).

<sup>6</sup>X. Gonze, P. Käckell, and M. Scheffler, Phys. Rev. B **41**, 12264 (1990).

<sup>7</sup>R. Stumpf, X. Gonze, and M. Scheffler, Fritz-Haber-Institut Research report, April 1990 (unpublished).

<sup>8</sup>G. A. Baraff and M. Schlüter, Phys. Rev. Lett. **55**, 1327 (1985).

<sup>9</sup>H. P. Hjalmarsen, P. Vogl, D. J. Wolford, and J. D. Dow, Phys. Rev. Lett. **44**, 810 (1980).

<sup>10</sup>M. Scheffler, in *Festkörperprobleme: Advances in Solid State Physics*, edited by P. Grosse (Vieweg, Braunschweig, 1982), Vol. XXII, p. 115.

<sup>11</sup>M. Scheffler, Physica (Amsterdam) **146B**, 176 (1987).

<sup>12</sup>H. Tanino and M. Tajima, Phys. Rev. B **33**, 5965 (1986).

<sup>13</sup>M. J. Caldas, J. Dabrowski, A. Fazzio, and M. Scheffler (to be published).

<sup>14</sup>A. Fazzio (to be published).

<sup>15</sup>W. C. Mitchell and P. W. Yu, J. Appl. Phys. **62**, 4781 (1987).

<sup>16</sup>The values for  $E_B = E_M - E_W$  and  $E_W$  are smaller than the values published in Refs. 1 and 3 due to the fact that in the older calculations we considered only the *s* nonlocality of the pseudopotential (see the discussion in Ref. 3). In the present calculations we use some technical improvements and separable nonlocal pseudopotentials (Refs. 6 and 7), taking different potentials for  $l=0, 1, \text{ and } 2$ . These numerical differences from our previous results do not change any of the previous conclusions.